

~~RESTRICTED~~

SECURITY INFORMATION

C. 2
RM A52K12

NACA RM A52K12

JAN 22 1953

~~CONFIDENTIAL~~



RESEARCH MEMORANDUM

TECHNIQUES FOR DETERMINING THRUST IN FLIGHT

FOR AIRPLANES EQUIPPED WITH AFTERBURNERS

By L. Stewart Rolls, C. Dewey Havill,
and George R. Holden

Ames Aeronautical Laboratory
Moffett Field, Calif.

CLASSIFICATION CANCELLED

Authority: NACA R7-3465 Date 1/14/53

By 2/27/53 - See 12/13/53

~~CLASSIFICATION CHANGED~~

To:

Confidential

By authority of J. W. Crowley Date 2/11/53
NACA R7-1742 EO 1050K/SM 28/12/21/53
CLASSIFIED DOCUMENT

This material contains information affecting the National Defense of the United States within the meaning of the espionage laws, Title 18, U.S.C., Secs. 793 and 794, the transmission or revelation of which in any manner to an unauthorized person is prohibited by law.

NATIONAL ADVISORY COMMITTEE
FOR AERONAUTICS

WASHINGTON

January 19, 1953

~~CONFIDENTIAL~~

~~RESTRICTED~~

NACA LIBRARY
LANGLEY AERONAUTICAL LABORATORY
Langley Field, Va.



NATIONAL ADVISORY COMMITTEE FOR AERONAUTICS

RESEARCH MEMORANDUM

TECHNIQUES FOR DETERMINING THRUST IN FLIGHT

FOR AIRPLANES EQUIPPED WITH AFTERBURNERS

By L. Stewart Rolls, C. Dewey Havill,
and George R. Holden

SUMMARY

An experimental technique has been developed which enables a determination of the net propulsive force acting on an afterburner-equipped airplane in flight. The thrust measurement is based on the variation of static and total pressure and stagnation temperature across the fuselage exit as determined by a swinging pitot-static pressure and temperature probe. The details are also presented for an air-cooled fixed-pressure probe for the determination of basic engine thrust.

INTRODUCTION

The need of research and development flight test groups for practical methods of measuring propulsive forces in flight has been greatly increased with the advent of high-power turbojet engines using afterburner-thrust augmentation. The necessity of providing large amounts of cooling air for both airframe and engine has resulted in complex engine installations of the type wherein it is very difficult either to assess the actual performance of the installed engine or to investigate suspected performance losses caused by the cooling-air flow without using detailed jet-exit mass-flow and momentum surveys. The very high jet temperatures (about 3500° F) accompanying afterburner operation prevent the use of conventional fixed survey instruments without using special materials that are prohibitively expensive and difficult to fabricate.

A power-operated moving probe has been developed at the Ames Aeronautical Laboratory and used successfully in flight tests to determine the variation of total and static pressure and stagnation temperature across the jet exit. These measurements are used to compute the gross and net thrust for a typical afterburner-equipped fighter airplane.

Measurements of the total pressure in the engine tailpipe with a fixed air-cooled probe, together with a knowledge of the air-flow rate through the engine, enabled the thrust produced by the engine alone to be determined. The difference between the thrust at the tailpipe plane and that at the jet exit (swinging probe) plane represents the ejector losses plus cooling air losses forward of the tailpipe plane. The isolation of the ejector losses requires, in addition, a survey to determine the momentum of the secondary air at the tailpipe exit plane.

This report presents a description of the test equipment and test techniques and some typical flight-test results to aid in application of the techniques by other interested flight test groups.

SYMBOLS

A	radial area, square feet
F_G	gross thrust, pounds
F_N	net thrust, pounds
g	gravitational acceleration, feet per second squared
k	constant
M	Mach number
p_T	local total pressure, pounds per foot squared
p_s	local static pressure, pounds per foot squared
p_0	free-stream static pressure, pounds per foot squared
q_c	dynamic pressure ($p_T - p_s$), pounds per foot squared
R	gas constant, pound-foot per pound $^{\circ}$ F
T_1	thermocouple temperature for zero time lag, $^{\circ}$ F
T_o	actual thermocouple temperature, $^{\circ}$ F
T_s	exhaust-gas static temperature, $^{\circ}$ F
V	airplane velocity, feet per second
W_a	air-flow rate, pounds per second
$\frac{W_a V}{g}$	total ram drag, pounds

γ ratio of specific heats, dimensionless
 θ time, seconds

GENERAL METHOD

A cross section of a typical jet-actuated ejector and fuselage exit is shown in figure 1. Normally, airplane performance testing has been based on either estimated or measured engine thrust in the primary system only. However, this procedure is not realistic if the use of large amounts of cooling air in the secondary system introduces appreciable thrust losses.

In order to determine the actual thrust for performance or airplane drag computations, it is necessary to measure the net propulsive thrust at the fuselage exit, indicated in figure 1 as the swinging probe survey station. In order to evaluate the losses in thrust due to the cooling-air flow (i.e., momentum losses in the cooling-air passage and mixing losses in the ejector nozzle), it is necessary to measure the primary thrust at the tailpipe exit plane or, if a clamshell is used, in the clamshell exit plane.

The desired net propulsive force can be defined as (see reference 1):

$$F_N = F_G - \frac{W_a V}{g} \quad (1)$$

The gross thrust term is obtained by integrating the point-to-point survey of the total and static pressures at the fuselage-exit plane using the expression

$$dF_G = \frac{2\gamma}{\gamma-1} p_s \left[\left(\frac{p_T}{p_s} \right)^{\frac{\gamma-1}{\gamma}} - 1 \right] dA - (p_s - p_o) dA \quad (2)$$

To compute the ram drag term in equation (1), it is necessary to measure the total air flow through the ejector system. This is done by computing the total weight flow rate of the primary exhaust gas plus cooling air using measured values of local static and total pressures and local stagnation temperature. It is then assumed that this weight flow is equal to the total air flow, which is equivalent to neglecting the weight of fuel in the primary stream. The air flow can then be computed using the following equation:

$$dW_a = \sqrt{\frac{2\gamma}{\gamma-1} \frac{g(p_s)^2}{RT_s} \left[\left(\frac{p_T}{p_s} \right)^{\frac{\gamma-1}{\gamma}} - 1 \right]} dA \quad (3)$$

For the specific case of the primary system, it is possible to simplify the gross-thrust equation (equation (2)) to:

$$\frac{F_G}{p_o A} = \frac{2\gamma}{\gamma-1} \left[\left(\frac{p_T}{p_s} \right)^{\frac{\gamma-1}{\gamma}} - 1 \right] \text{ for } \frac{p_T}{p_o} < \left(\frac{\gamma+1}{2} \right)^{\frac{\gamma}{\gamma-1}} \quad (4)$$

$$= \frac{2p_T}{p_o} \left(\frac{2}{\gamma+1} \right)^{\frac{1}{\gamma+1}} - 1 \text{ for } \frac{p_T}{p_o} \geq \left(\frac{\gamma+1}{2} \right)^{\frac{\gamma}{\gamma-1}} \quad (5)$$

In the derivation of equations (4) and (5), it is assumed that there is a uniform distribution of pressure across the tailpipe and that the static pressure in the nonchoked nozzle case was equal to free-stream static pressure. To compute the net thrust produced by the primary jet, it is necessary to know the engine air-flow rate. Three available methods are: (1) computation from engine operating conditions and engine manufacturer's data on the compressor, (2) computation from measured tailpipe total and static pressures and temperature, and (3) measurement of the air-flow rate at the engine air inlets. The first method was used in the present tests.

EQUIPMENT AND INSTRUMENTATION

Primary Gross-Thrust Measurement

The fixed total-pressure probe used to measure the primary thrust is shown in figure 2. The dimensions are shown in figure 3. Since this probe is in the exhaust continuously, it is cooled by air bled from the engine compressor. For this purpose, a line 1-1/2 inches in diameter was connected to the cockpit pressurizing and refrigerating system. The average life for a fixed probe was about 6 hours, of which approximately 45 minutes was during afterburner operation. Occasionally cracks appeared on the vertical support member which were welded between flights. These probes are now being sprayed with aluminum under oxidizing conditions, such that approximately 25 percent of the coating is aluminum oxide. Preliminary results of the coated probes indicate that the life of the probes will be prolonged.

Total Gross-Thrust Measurements

The thrust of the over-all ejector system is evaluated using equation (2) with the total and static pressures measured by the power-operated swinging probe shown mounted on the airplane in figure 4. Figure 5 is an exploded view showing the type of construction used. Although the swinging probe was originally air cooled, it was found that the probe was not in the exhaust stream long enough to require cooling. The actuator on the probe was adjusted so that the time required to traverse the jet was approximately 4 seconds. The pitot-static pressure probe was calibrated in the Ames 2- by 2-foot transonic test equipment. The results of the static-pressure calibration of this probe are presented in figure 6.

The differential-pressure transmitters used are Statham's Model P22A which has a range of 15 pounds per square inch. A total-pressure tube was mounted atop the vertical fin of the airplane to supply a reference pressure for these total- and static-pressure transmitters. This reference pressure was recorded by a 0 to 15 pounds per square inch absolute pressure transmitter. The transmitters for the swinging probe were mounted close to the probe so as to minimize the time lag in the tubing system. The time lag constants (reference 2) for the pressure systems are 0.01 second for the static pressures and 0.025 second for the total pressures. The probe position transducer used was a Heliopot Model G. A total of approximately 400 traverses of the jet have been made with this probe, of which approximately 50 were made with the afterburner operating. The probe does not show any ill effects from the hot exhaust gas.

Total Air-Flow Measurements

To determine the rate of air flow through the ejector system by means of equation (3), it is necessary to know the variation of static temperature across the fuselage exit. The local static temperature can be obtained from measurements of the local stagnation temperature and local total and static pressures. To determine the local stagnation temperature a Chromel-Alumel thermocouple was mounted on the vertical member of the swinging probe as shown in figure 5. These temperatures were recorded on a rapid-acting self-balancing potentiometer. The time constant for the recording system is 0.03 second. The recorded temperature from this thermocouple was used with the following equation to determine the local stagnation temperature profile:

$$[(T_1 - T_0) + 0.168 \frac{d}{d\theta} (T_1 - T_0)]^2 = 1500 \frac{dT_0}{d\theta} \quad (6)$$

The derivation of this equation is presented in the appendix.

The method by which the swinging thermocouple was calibrated involves several assumptions concerning the temperature measurements. It is assumed that during ground tests with afterburner off, the probe, when held stationary in the jet, records the true local stagnation temperature of the gas. For the range of temperature encountered under these conditions, it has been calculated that the thermocouple error due to radiation losses is small - of the order of 1 percent of the local absolute temperature. As a further check on the validity of this measurement, it is noted that the measured jet center-line temperature was in good agreement with the standard thermocouple used to indicate the airplane tailpipe temperature.

The thermocouple is then swung through the jet and the transient measurement of temperature is empirically related to the previously measured steady-state temperature profile. The most drastic assumption, however, is that the relation between the transient and steady-state temperature, which is determined for the case of afterburner-off operation, holds without modification for the case of afterburner-on operation. For the case of afterburner-on operation, the maximum jet temperature is approximately three times the jet temperature during afterburner-off operation, consequently radiation effects are much more severe. At this time, insufficient data are available to determine the magnitude of the error involved by this assumption; however, calculations indicate that for the case of afterburner-on operation, the error in the maximum jet temperature due to radiation losses from the swinging probe does not exceed 10 percent. An error of this magnitude causes an error of approximately 5 percent in the integrated value of net thrust. Refinements in the temperature measuring technique are currently under development.

In order to eliminate the speed at which the swinging probe was moved across the jet as a variable, the speed was held constant for all tests.

Precision of Measurements

The precision of the measurements based on the least count on the instruments and upon the scatter and repeatability of the data are:

p_T	± 5 lb per ft^2
p_S	± 5 lb per ft^2
p_o	± 5 lb per ft^2
$\frac{F_G}{A}$ (afterburner off)	± 30 lb per ft^2
$\frac{F_G}{A}$ (afterburner on)	± 37 lb per ft^2

~~RECORDED~~

Radial position	$\pm 1/8$ in.
$\frac{W_a}{A}$ A (afterburner off)	± 0.3 lb per sec per ft^2
$\frac{W_a}{A}$ A (afterburner on)	± 0.6 lb per sec per ft^2

TYPICAL TEST DATA

A typical set of data obtained during flight tests of an afterburner-equipped fighter airplane is presented in figure 7. The variations of total pressure, static pressure, and stagnation temperature are shown as a function of radial position at the fuselage exit. The free-stream static pressure is also shown in the figure as a reference. By use of the methods of this report, these profiles have been used to compute the local gross-thrust and net-thrust variations across the fuselage exit. These results are shown in figure 8. The total gross- and net-propulsive force can be determined by integrating the curves shown in figure 8 over the total area of the fuselage exit. The values of total gross and net thrust obtained from integrating these curves are shown in figure 8.

CONCLUDING REMARKS

A technique has been developed which enables measurement of the propulsive force on airplanes equipped with afterburners. The test equipment enables the gross thrust and the air-flow rate at the exit of the fuselage to be computed. These data enable the net thrust to be determined with an over-all accuracy of about 5 percent at the full power condition.

Ames Aeronautical Laboratory
National Advisory Committee for Aeronautics
Moffett Field, California

APPENDIX

TEMPERATURE CALIBRATION

The method used to calibrate the swinging-probe thermocouple was as follows. The steady-state temperature profile across the jet exit was first established by means of ground tests. The probe was held at various fixed positions in the jet, and the temperature recorded after the thermocouple temperature had reached equilibrium at each position. A typical temperature profile is shown in figure 9. The thermocouple was then swung through the jet and its response recorded. Figure 10 shows a typical thermocouple response (T_o) and also the response which a thermocouple with zero time lag would have (T_i). In this figure, the curve labeled T_i was obtained from figure 9 and a knowledge of probe position as a function of time.

In order to relate the transient temperature as indicated by the swinging probe to the previously established steady-state temperature, the following relation was assumed:

$$\frac{dT_o}{d\theta} = f \left[(T_i - T_o) + k \frac{d}{d\theta} (T_i - T_o) \right] \quad (A1)$$

To determine the functional relation shown in equation (A1), experimental values of $(T_i - T_o)$ and $d/d\theta(T_i - T_o)$ were plotted as a function of $dT_o/d\theta$, as shown in figure 11. From this figure, it can be seen that for any value of $dT_o/d\theta$ two values of $(T_i - T_o)$ and $d/d\theta(T_i - T_o)$ exist.

Thus, equation (A1) can be written as

$$f \left[(T_i - T_o)_1 + k \frac{d}{d\theta} (T_i - T_o)_1 \right] = f \left[(T_i - T_o)_2 + k \frac{d}{d\theta} (T_i - T_o)_2 \right] \quad (A2)$$

where the subscripts 1 and 2 indicate values of the variables obtained for a given value of $dT_o/d\theta$. Substitution of experimental values for $(T_i - T_o)$ and $d/d\theta(T_i - T_o)$ for any value of $dT_o/d\theta$ yields a numerical value of k . Values of k are then plotted as a function of $dT_o/d\theta$ as shown in figure 12. The final value chosen by inspection of these data was 0.168. Knowing k then, the function in equation (A1) is determined by plotting $(T_i - T_o) + 0.168 d/d\theta(T_i - T_o)$ as a function of $dT_o/d\theta$. The final relationship shown by the faired curve in figure 13 corresponds to equation (6).

REFERENCES

1. Pyle, Raymond W.: Determination of Turbojet Engine Thrust from Tailpipe Measurements. Jour. Aero. Sci., vol. 14, no. 10, Oct. 1947, p.561.
2. Huston, Wilber B.: Accuracy of Airspeed Measurements and Flight Calibration Procedures. NACA Rep. 919, 1948.

~~RESTRICTED~~

NACA RM A52K12

~~RESTRICTED~~

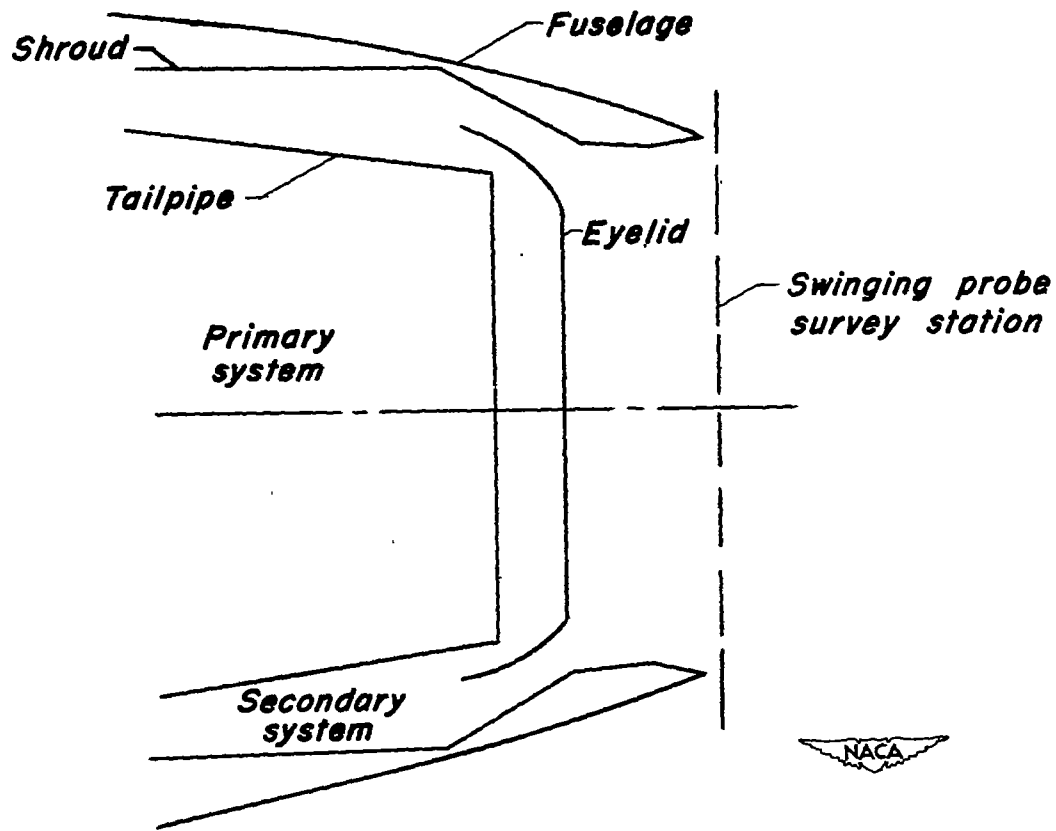


Figure 1.— Cross section of a typical jet-actuated ejector and fuselage exit.

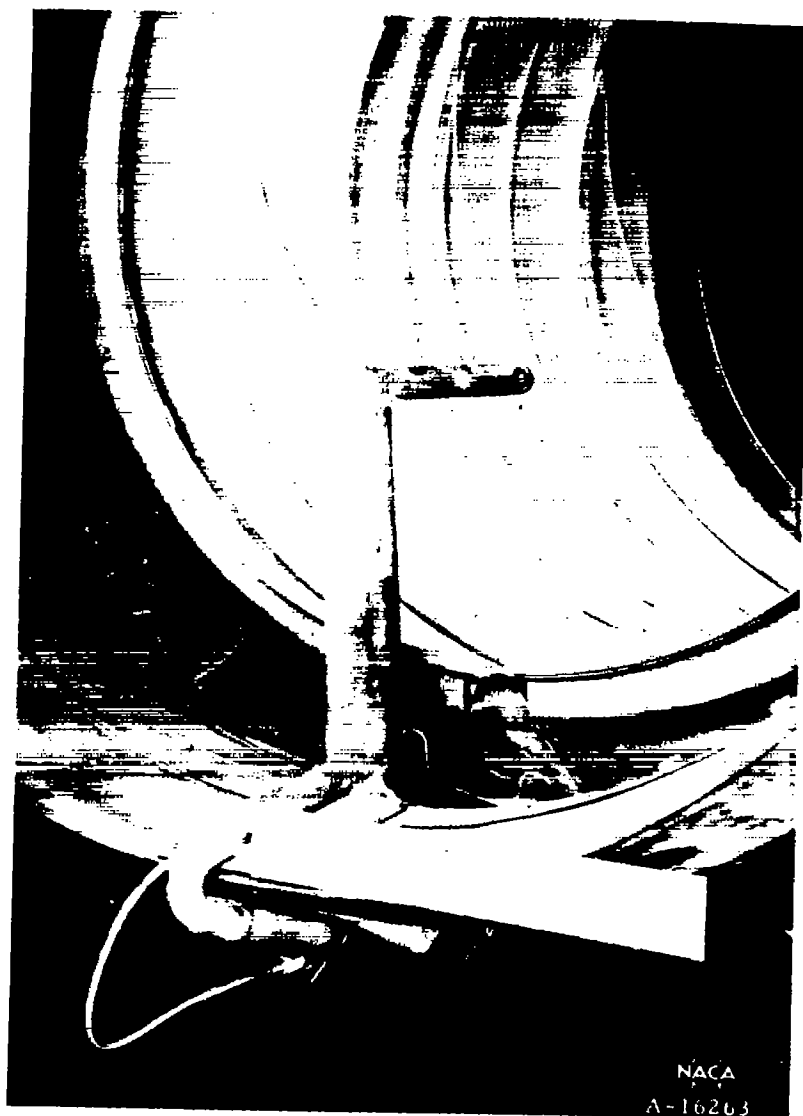


Figure 2.— Fixed, air-cooled, total-pressure probe used to measure primary thrust.

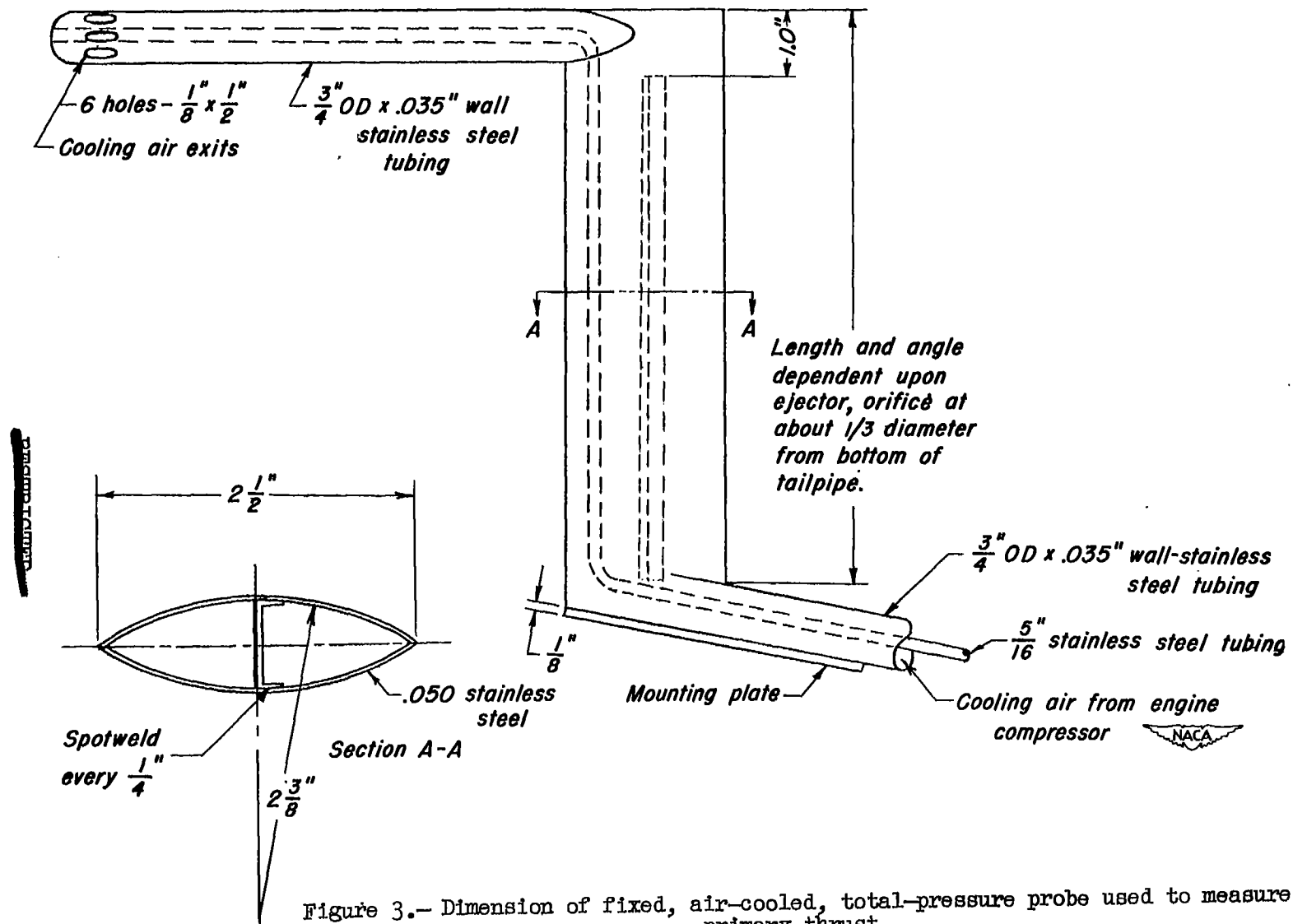


Figure 3.— Dimension of fixed, air-cooled, total-pressure probe used to measure primary thrust.



Figure 4.— View of swinging probe and stationary probe mounted on airplane.

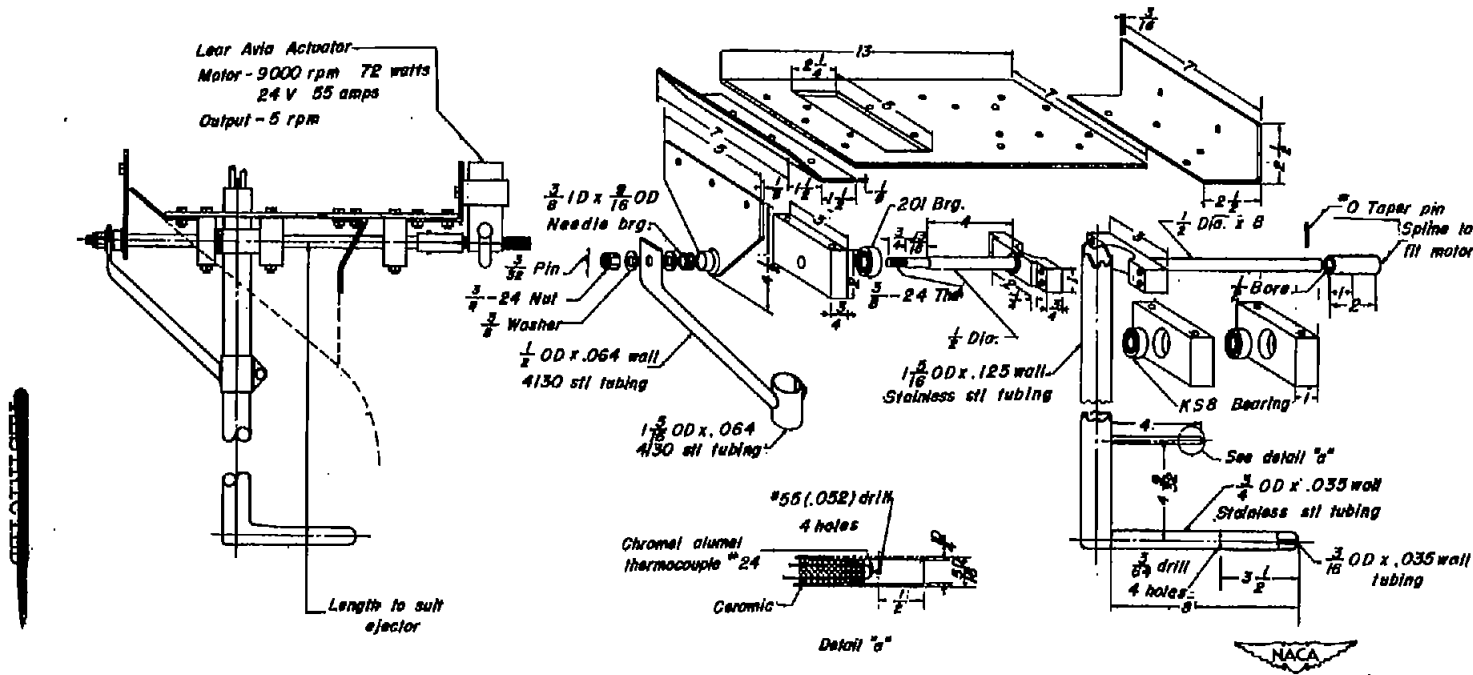


Figure 5.- Exploded view of swinging probe.

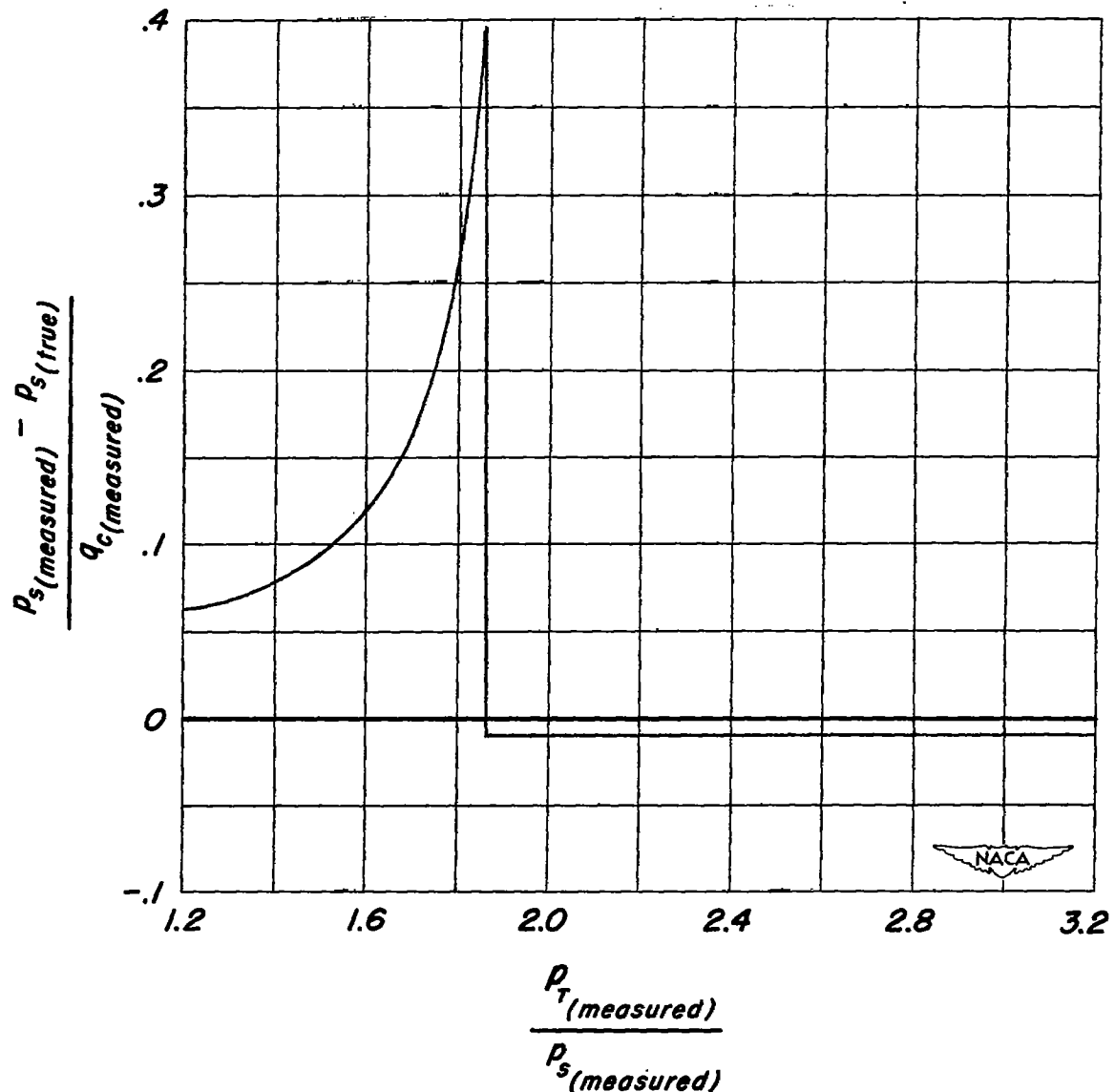


Figure 6.— Calibration of the swinging pitot-static pressure probe as determined in the Ames 2- by 2-foot transonic test equipment.

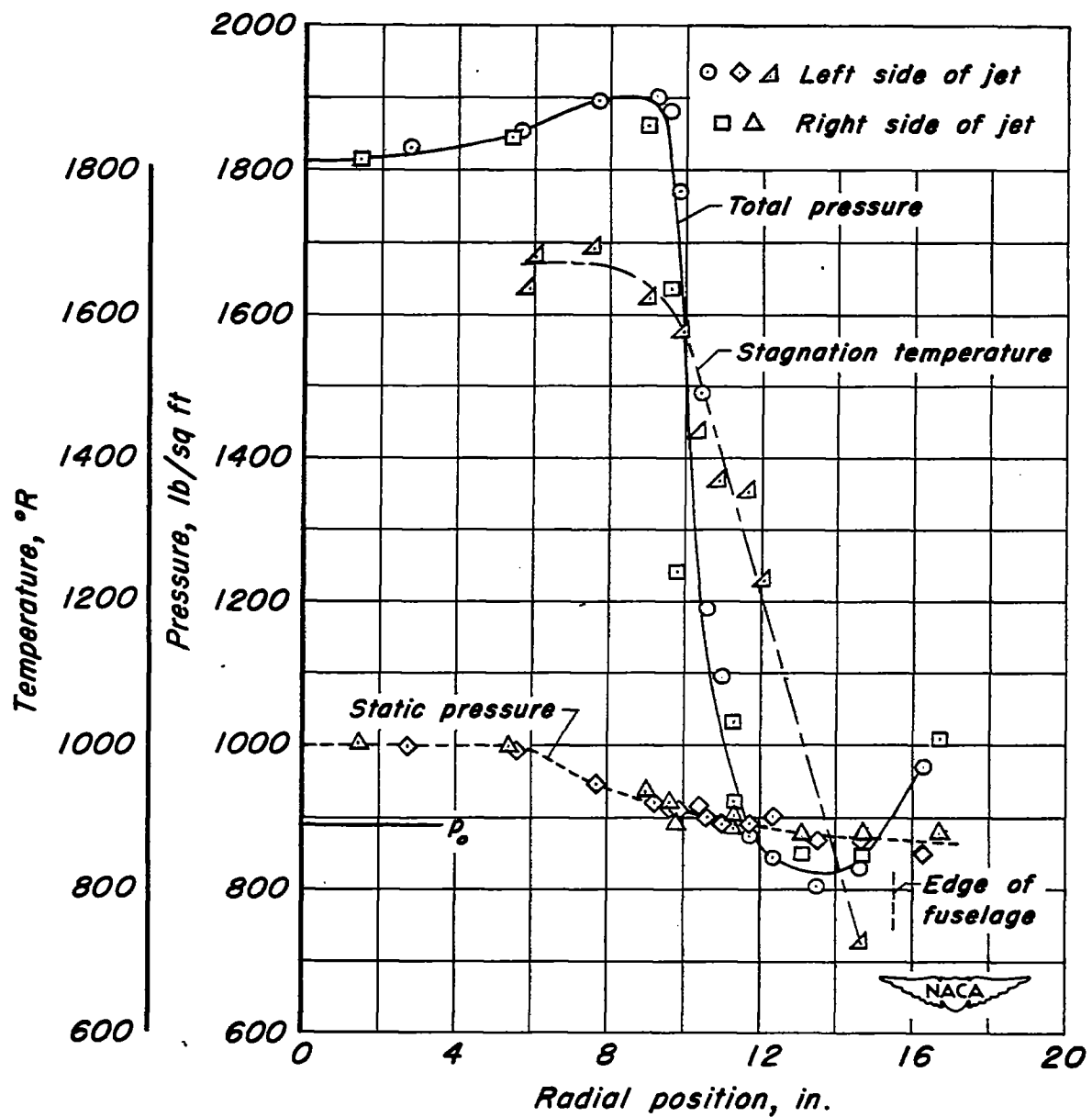
(a) $M = 0.76$, afterburner off.

Figure 7.— Typical pressure and temperature profile across the fuselage.

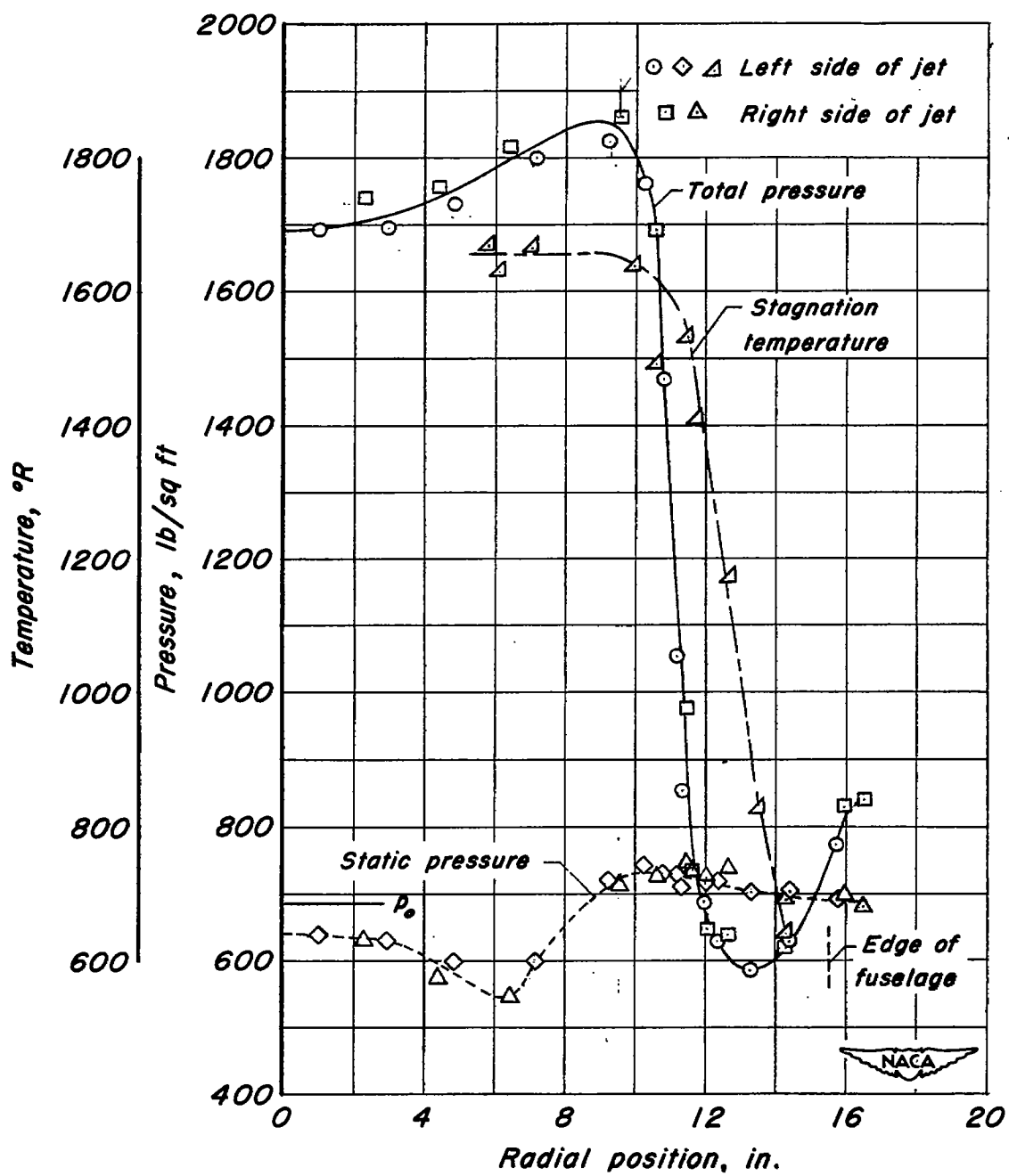


Figure 7.—Continued.

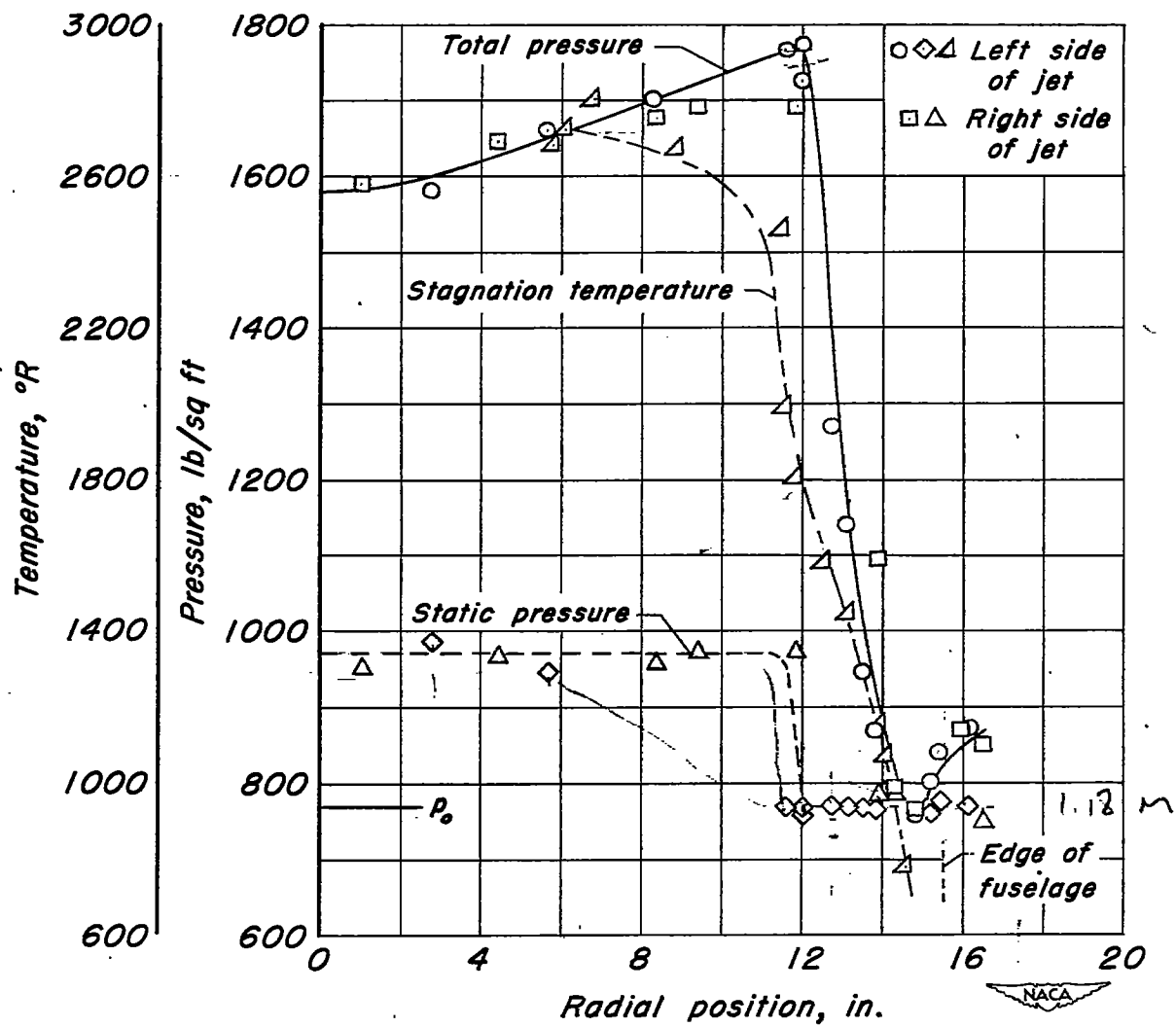
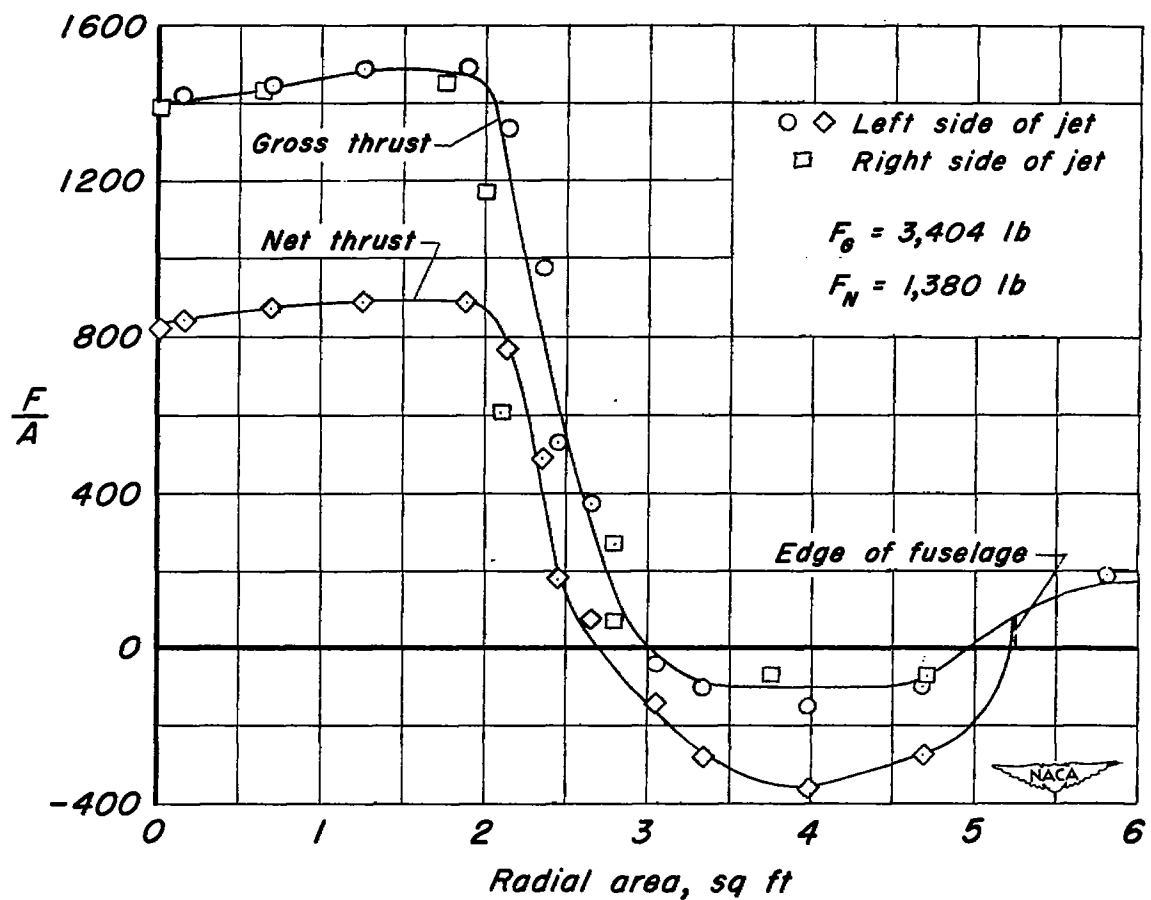
(c) $M = 0.76$, afterburner on.

Figure 7.— Concluded.



(a) $M = 0.76$, afterburner off.

Figure 8.— Typical thrust profiles across the fuselage exit.

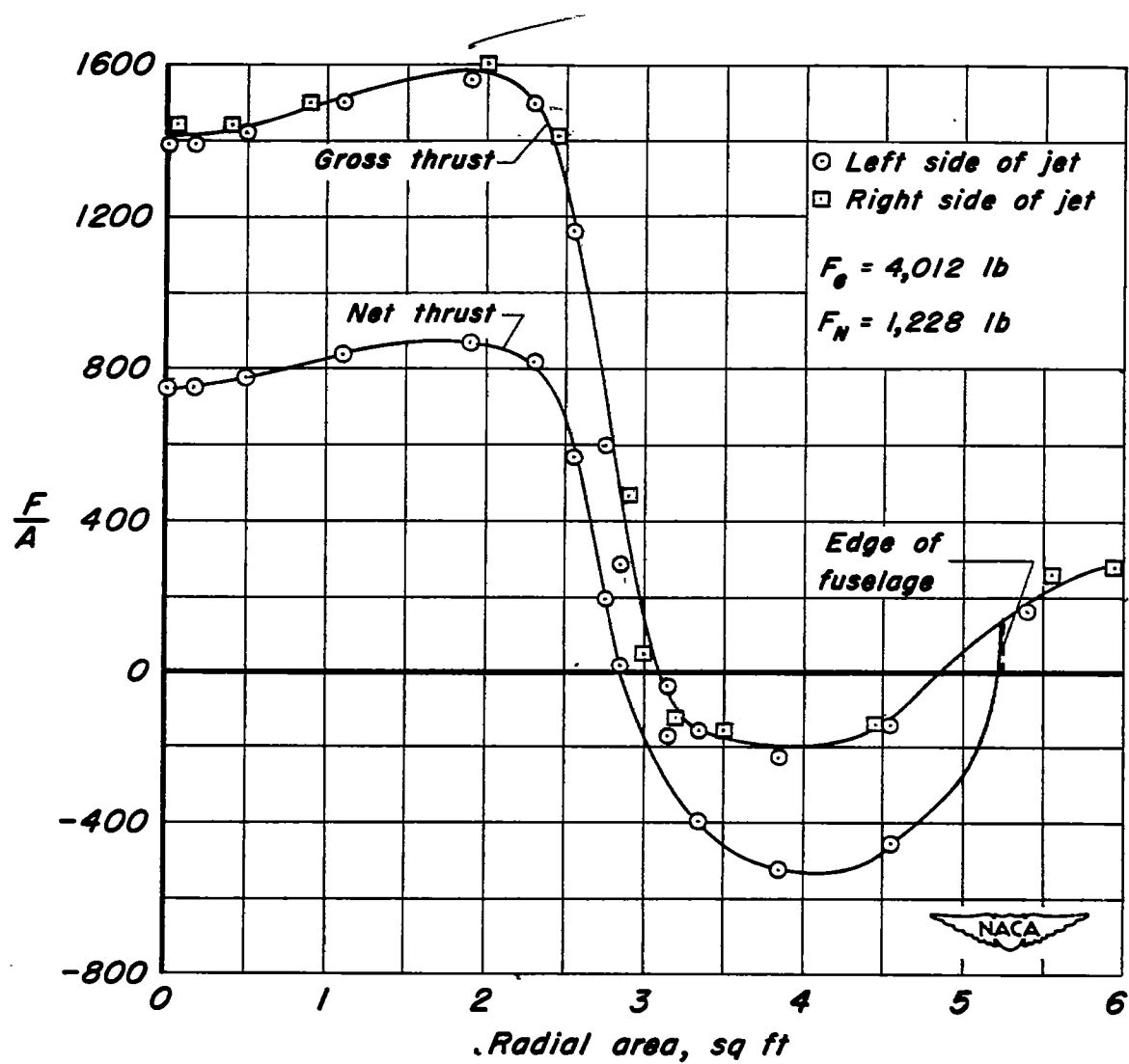
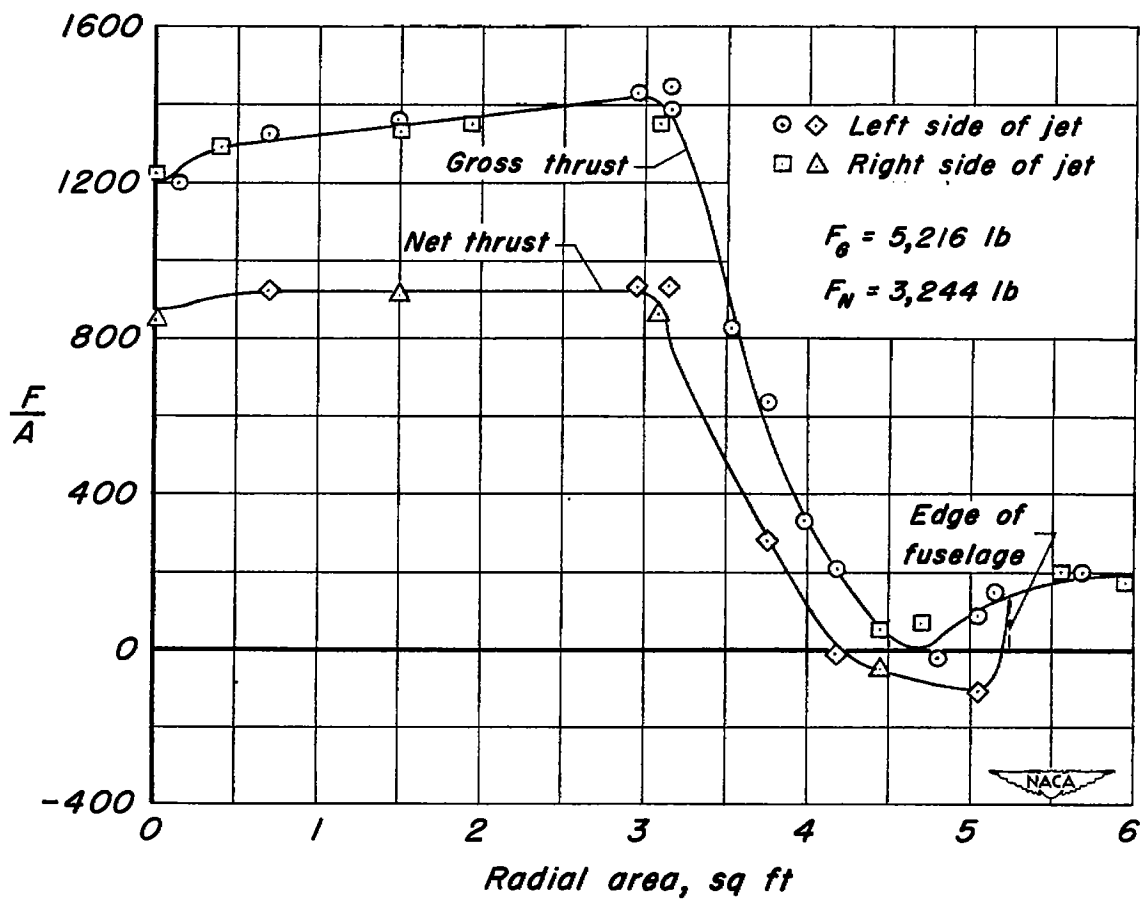
(b) $M = 0.97$ afterburner off.

Figure 8.—Continued.



(c) $M = 0.76$, afterburner on.

Figure 8.— Concluded.

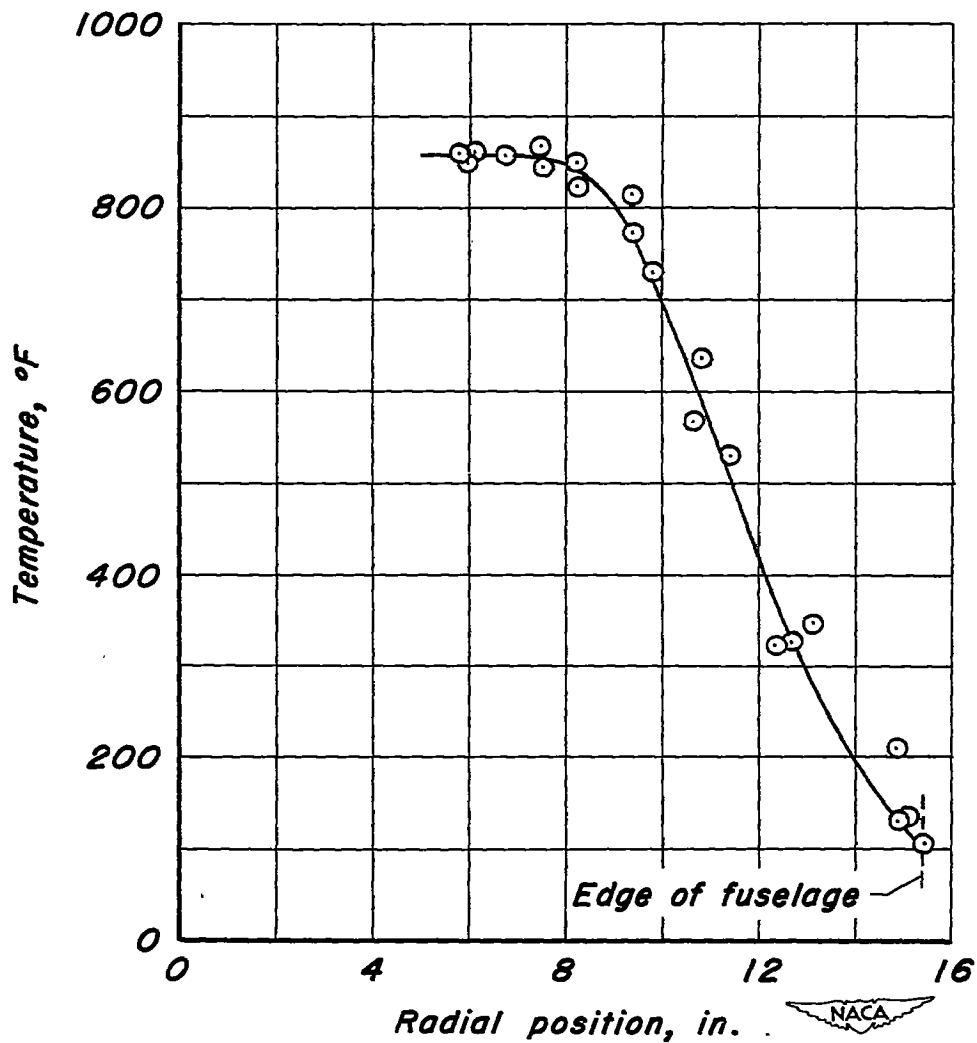


Figure 9.— Temperature profile across the jet exit.

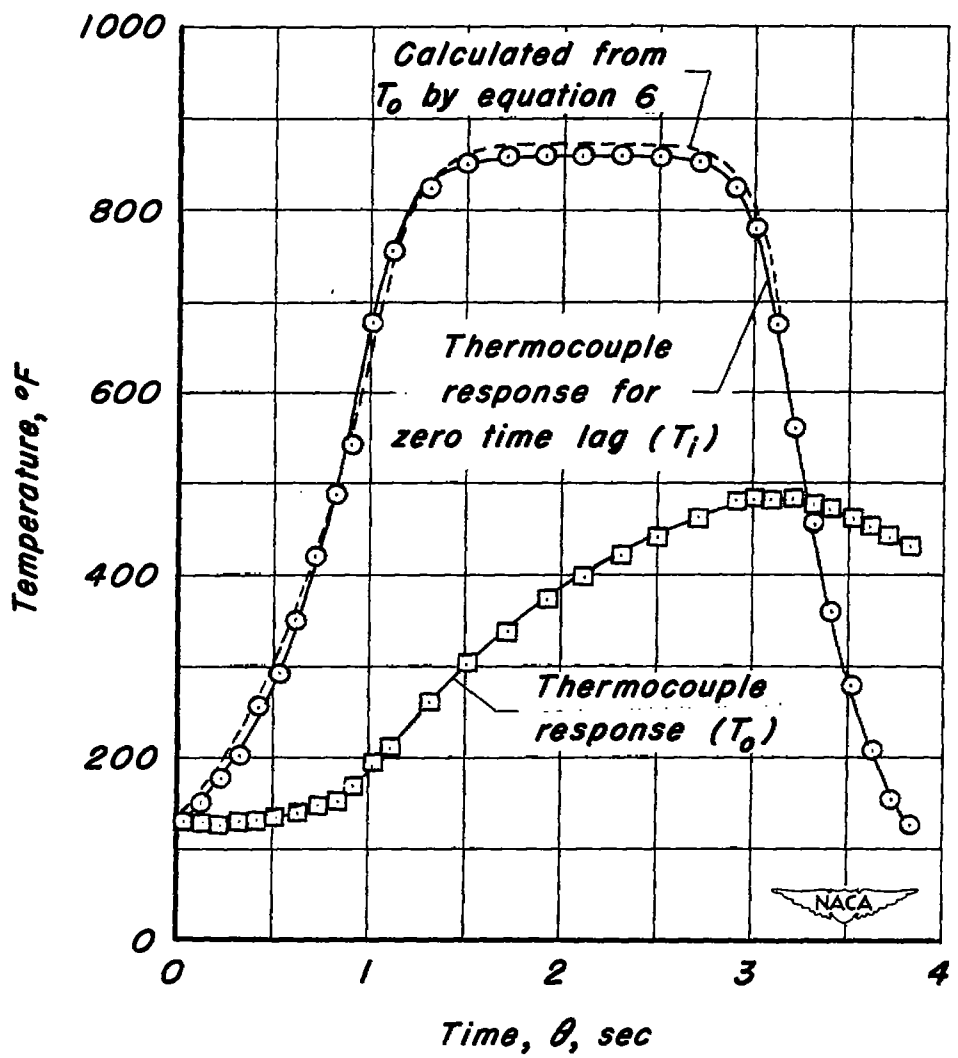


Figure 10.— Thermocouple response versus time.

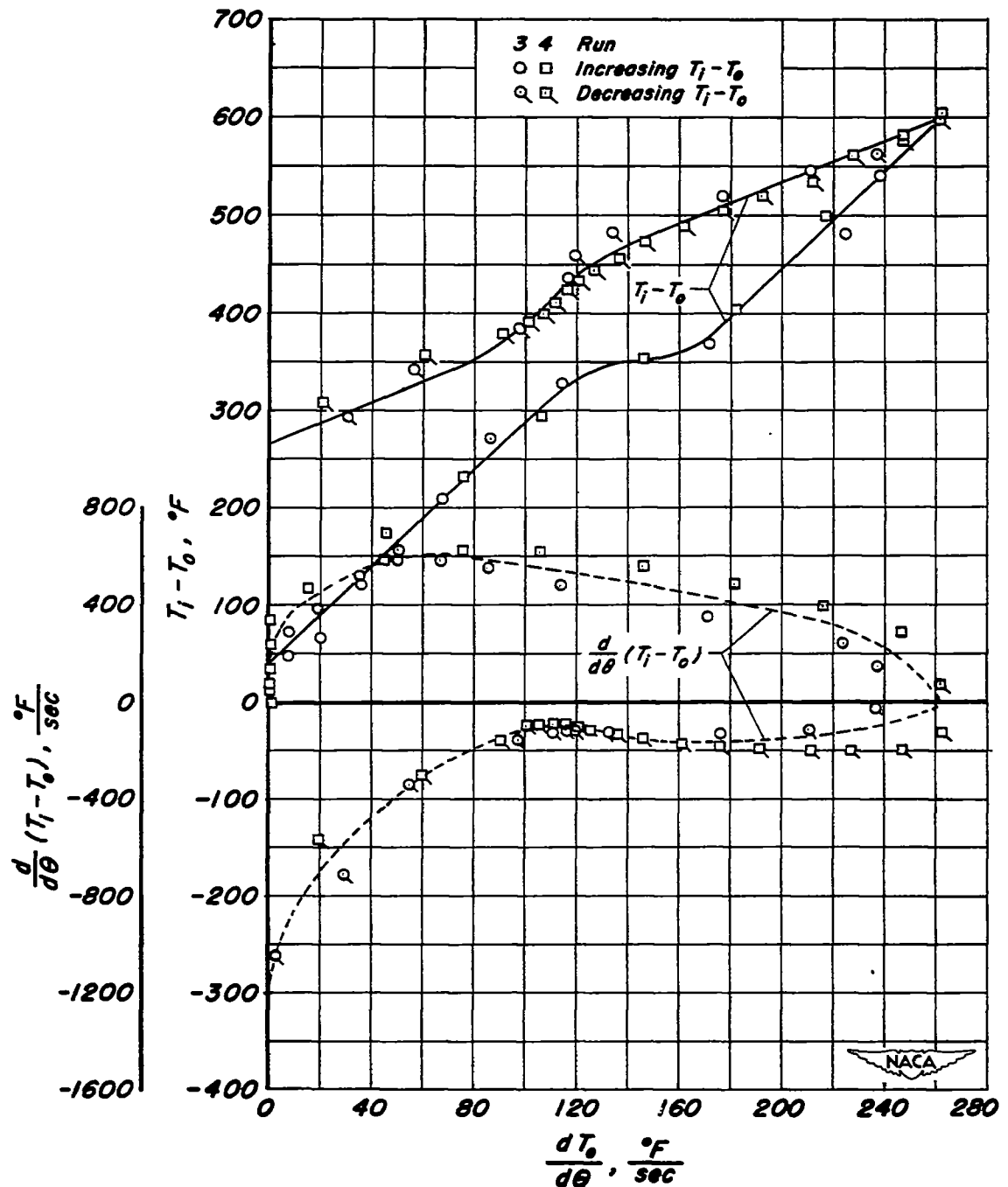


Figure 11.—Variation of $(T_i - T_0)$ and $\frac{d}{d\theta}(T_i - T_0)$ with $\frac{dT_0}{d\theta}$ as determined in ground tests.

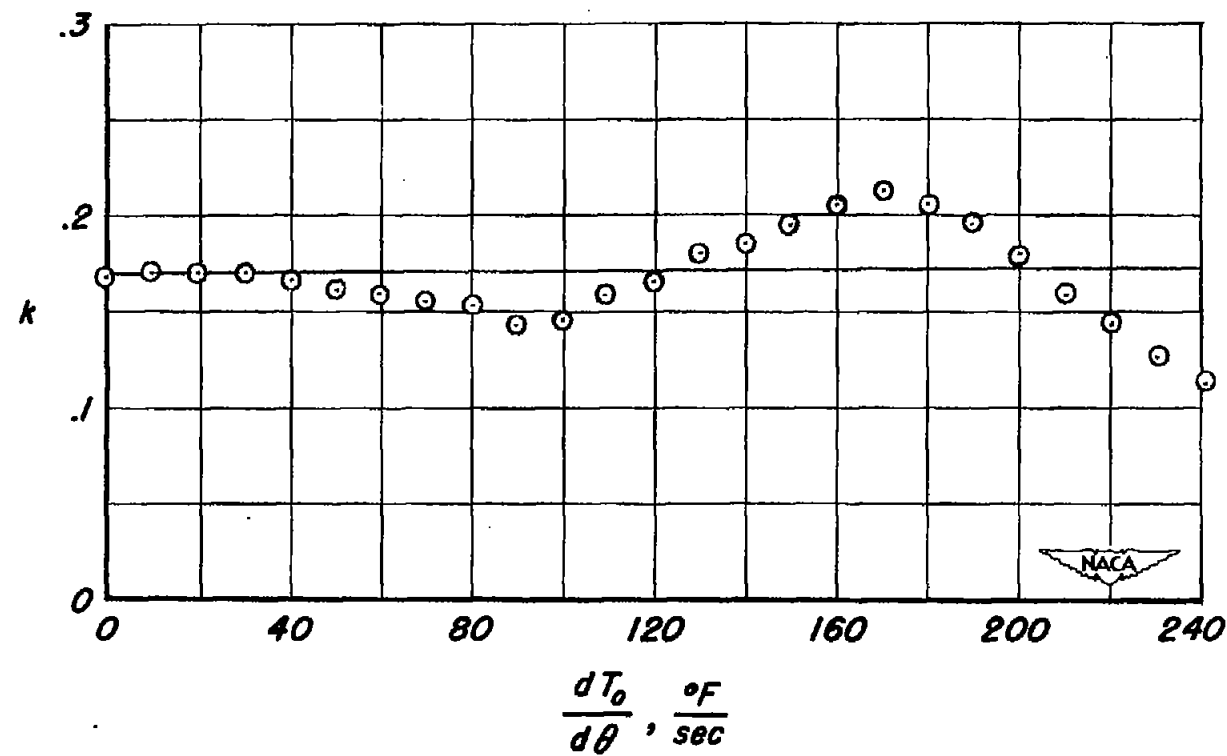
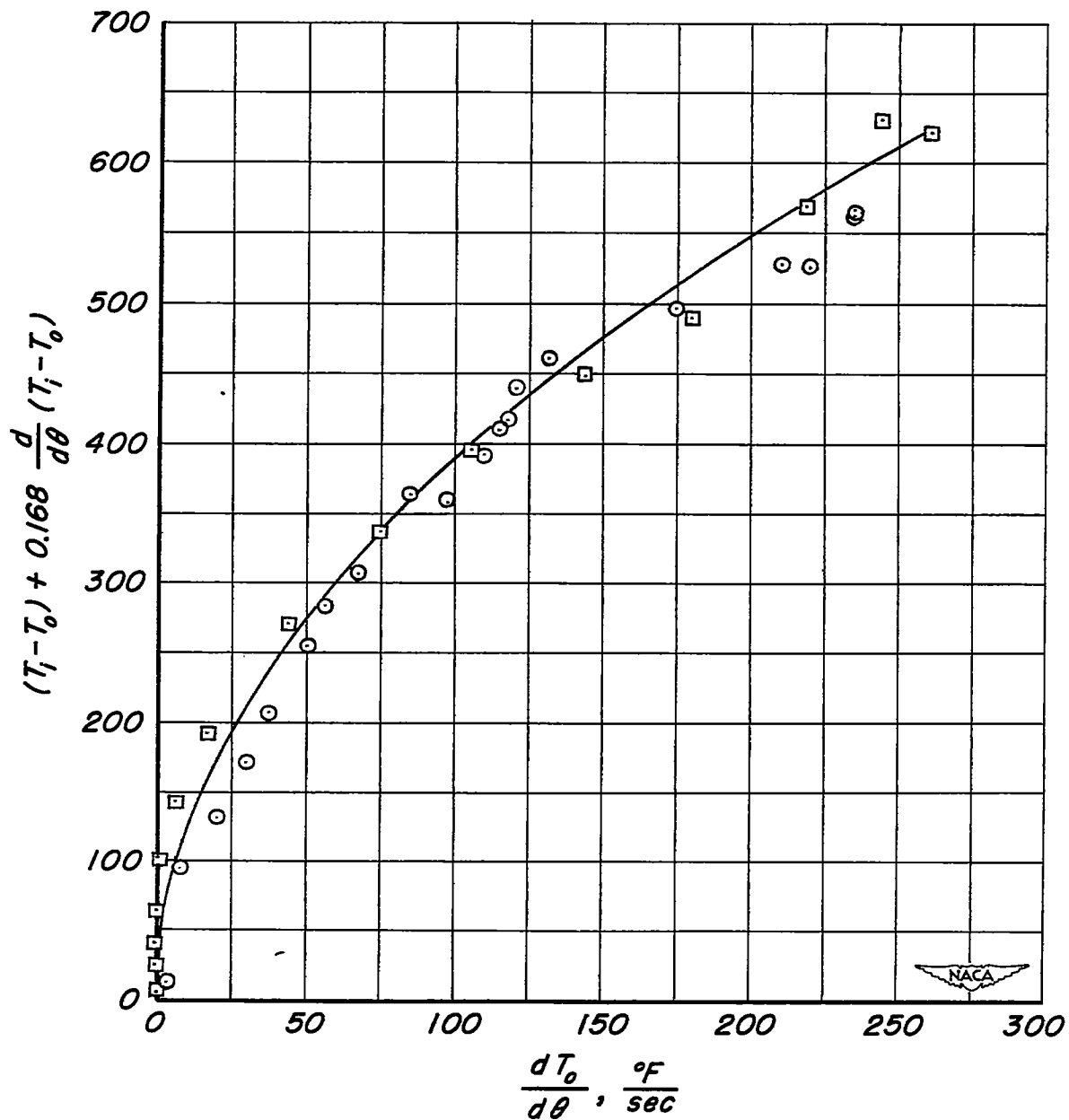


Figure 12.—Variation of k with $\frac{dT_0}{d\theta}$.

Figure 13.— Curve establishing relationship between T_i and T_0 .

SECURITY INFORMATION



3 1176 01434 8149

[REDACTED]

[REDACTED]